ORIGINAL ARTICLE

Long-term intensive training induced brain structural changes in world class gymnasts

Ruiwang Huang · Min Lu · Zheng Song · Jun Wang

Abstract Many previous studies suggested that both short-term and long-term motor training can modulate brain structures. However, little evidence exists for such brain anatomical changes in top-level gymnasts. Using diffusion-weighted and structural magnetic resonance images of the human brain, we applied voxel-based morphometry (VBM) and tract-based spatial statistics (TBSS) as well as FA-VBA (voxel-based analysis of fractional anisotropy, a VBM-style analysis) methods to quantitatively compare the brain structural differences between the world class gymnasts (WCG) and the non-athlete groups. In order to reduce the rate of false positive findings, we first determined that the clusters defined at a threshold of $t > 2.3$ and a cluster significance of $p < 0.05$ (FWE-corrected) across all subjects were the brain regions that showed significant differences in a between-group comparison. We then constructed several between-group comparisons based on the repeated diffusion or structural MRI data and created the intersecting regions from multiple between-group comparisons. Thus, we found significantly decreased fractional anisotropy (FA) not only in the white matter of the WCG in areas that included the bilateral superior longitudinal fasciculus, inferior longitudinal fasciculus, and inferior occipito-frontal fascicle, but also in the gray matter of the WCG in areas that included the bilateral middle cingulum, bilateral postcentral gyri, and bilateral motor regions. We also identified significantly increased gray matter density in the WCG, especially in the left inferior frontal gyrus, bilateral inferior and superior parietal lobule, bilateral superior lateral occipital cortex, left cuneus, left angular gyrus, and right postcentral gyrus. We speculate that the brain changes of the WCG may reflect the gymnasts' extraordinary ability to estimate the direction of their movements, their speed of execution, and their identification of their own and surrounding objects' locations. Our findings suggest that our method of constructing intersecting regions from multiple between-group comparison can considerably reduce the false positives, and our results provide new insights into the brain structure changes induced by long-term intensive gymnastic training.

Keywords Gray/white matter · Fractional anisotropy · Neuroplasticity · Morphology · Overlapping/intersecting regions

R. Huang · M. Lu · Z. Song · J. Wang (✉)
State Key Laboratory of Cognitive Neuroscience and Learning,
Beijing Normal University, Beijing 100875,
People's Republic of China
e-mail: Jun_Wang@bnu.edu.cn

R. Huang (✉)
Brain Imaging Center, Center for Studies of Psychological
Application, Key Laboratory of Mental Health and Cognitive
Science of Guangdong Province, School of Psychology,
South China Normal University, Guangzhou, 510631,
People's Republic of China
e-mail: ruiwang.huang@gmail.com

M. Lu
Key Laboratory of Mental Health, Institute of Psychology,
Chinese Academy of Sciences, Beijing 100101,
People's Republic of China

Abbreviations

DTI	Diffusion tensor imaging
FA	Fractional anisotropy
GM	Gray matter
WM	White matter
FA-VBA	Voxel-based analysis of FA

WCG	World class gymnasts (Gymnastic World Champions or Olympics Champions)
MRI	Magnetic resonance imaging
TBSS	Tract-based spatial statistics
VBM	Voxel-based morphometry
GLM	General linear model
BA	Brodmann's area

Introduction

The outstanding performances of world class gymnasts (WCG) cause audiences to wonder how gymnasts' brain structure and function differ from those of non-athletes. One approach to answering these questions involves measuring the brain structures of WCG and comparing the results with those of non-athletes. The development of magnetic resonance imaging (MRI) techniques has provided tools that can be used to uncover plastic changes in human brain structure induced by intensive motor training (Draganski et al. 2004), learning new skills (Mechelli et al. 2004; Schmithorst and Wilke 2002), or neuropathological adaptation (Keller and Just 2009; Oh et al. 2009).

Structural plasticity or neuroplasticity is an intrinsic property of the human brain and enables people to achieve their best behavioral performance under a variety of conditions (Pascual-Leone et al. 2005). Neuroplasticity refers to the capacity of the nervous system to adapt or regenerate to modify the organization of the brain's structure and function in response to experience (Pascual-Leone et al. 2005). Previous studies suggested that both short-term (Scholz et al. 2009; Draganski et al. 2004) and long-term training (Gaser and Schlaug 2003; Bengtsson et al. 2005; Hänggi et al. 2010; Jäncke et al. 2009b) can modulate structural changes in the brain gray matter (GM) and white matter (WM). Gaser and Schlaug (2003) revealed that professional pianists had higher GM density in the motor, auditory, and visual-spatial regions than non-pianists. In addition, Bengtsson et al. (2005) showed that pianists had a higher FA than non-pianists in the brain WM of the corticospinal tract; but, more interestingly, they also showed that the FA in this tract and in other pathways, such as the corpus callosum and arcuate fasciculus, correlated positively with the amount of time spent practicing the piano. Their results also suggested that the WM responds to practice and that different pathways have different sensitive periods during development. Hänggi et al. (2010) reported a decreased FA value in the brain WM of professional ballet dancers. Jäncke et al. (2009b) showed that skilled golfers exhibited smaller WM volumes and FA values in the internal and external capsule and in the parietal operculum, but larger GM volumes in the fronto-parietal network. Moreover,

Draganski et al. (2004) observed GM density changes in the bilateral mid-temporal areas and in the left posterior intra-parietal sulcus after short-term juggling practice. Scholz et al. (2009) detected an increased FA value in the WM underlying the right posterior intraparietal sulcus and increased GM density in the medial occipital and parietal lobe in a juggling learner group. Given the evidence from these studies, we attempted to construct intersecting regions from multiple between-group comparisons to pinpoint significantly changed brain regions in the WCG and to test the hypothesis that long-term intensive gymnastic training can also induce morphological changes in both brain GM and WM.

Voxel-based morphometry (VBM) (Ashburner and Friston 2000), tract-based spatial statistics (TBSS) (Smith et al. 2006), and voxel-based analysis of fractional anisotropy (FA-VBA, a VBM-style analysis) (Jones et al. 2005) analyses have increasingly become essential tools for investigating changes in brain structure (Benedetta et al. 2009; Good et al. 2001; Zatorre et al. 2012; Scholz et al. 2009). Usually, changes in brain structure have been reported from a single between-group comparison. However, whether the finding of brain structural changes is repeatable or reproducible has often been ignored, though the processing steps and methodological options, such as parameter choices, have been clearly described (Thomas et al. 2009; Ridgway et al. 2008; Mechelli et al. 2005). Several studies reported brain structural changes in different groups of healthy people after participating in 2–3 h training per day for several, e.g. 3–7, days (see the examples listed in a table in a paper written by Thomas and Baker 2013a). We were curious to learn whether the results from these studies were reliable or reproducible (Thomas et al. 2009; Jones et al. 2005). In principle, the idea that the same experiments always get the same results, no matter who performs them and how they perform them, is one of the cornerstones of scientific studies', including those on brain structural alteration, claim to objective truth. In this study, we first show that a large number of false positives are very likely to be obtained from brain structural studies if the conclusions are only based on a single between-group comparison. Then we present a method, in which we constructed intersecting regions from multiple between-group comparisons to identify significant alterations, thus reducing the number of false positives (Silver et al. 2011; Scarpazza et al. 2013). By using the proposed method on the MRI data acquired from the world-class gymnastic champions, our goal was to show that, compared with the intersecting regions derived from multiple between-group comparisons, the alterations determined from a single between-group comparison is vulnerable to false positives. Our final goal was to detect alterations in the brain

Table 1 Characteristics of the world class gymnasts who participated in this study

Champions	Discipline	Best medal records since 2007	Gender	Age (years)	Age of commencement (years)	Years of training (years)
1	Pommel horse	OC	M	24	4.5	19.5
2	Still rings	WC	M	24	4.5	19.5
3	Parallel bars	WC	M	23	4.5	18.5
4	Horizontal bar, AA	WC	M	26	4.5	21.5
5	Vault	OC	F	21	4.5	16.5
6	Uneven bars, AA	WC	F	17	4.5	12.5
7	Uneven bars, AA	OC	F	18	3.5	14.5
8	Floor exercises	OC	F	17	4.5	12.5
9	Uneven bars, AA	OC	F	17	4.5	12.5
10	Parallel bars, AA	WC	M	21	4.5	16.5
11	Uneven bars, AA	WC	F	19	4.5	14.5
12	Pommel horse	WC	M	23	4.5	18.5
13	Balance beam, AA	OC	F	17	4.5	12.5
Mean ± SD				20.5 ± 3.3	4.4 ± 0.3	16.1 ± 3.3

All of them have won individual or team gold medals in the Gymnastic World Championships or the Olympic Games since 2007 (*OC* Olympic Champions, *WC* World Champions or World-Cup Champions). The second column represents the dominant discipline for each of the champion subjects

AA all around

WM and GM in the world-class gymnastic champions. Because they had undergone long-term intensive training, we believed that alterations in their brains should be more easily detected than alterations in normal people who had only undergone a short period of training.

Previously, we investigated the topological properties of the human brain anatomical networks in a WCG group and compared their differences from the control group (Wang et al. 2013). In this study, one of our goals was to present a method of using the intersecting regions derived from multiple between-group comparisons to reduce false positives in the brain structural studies, and the other was to detect structural changes in brain GM and WM induced by long-term intensive gymnastic training in the WCG. We employed VBM to measure between-group differences in brain GM density, TBSS to estimate between-group differences in the FA of the brain WM, and FA-VBA to evaluate between-group differences in the FA of the brain GM. A nonparametric permutation test (Nichols and Holmes 2002) was applied to detect significant differences in brain structure between a group of WCG and a group of non-athlete controls. In order to reduce false-positive findings, we accepted only those intersecting regions that we were able to derive from multiple between-group comparisons to indicate the location and size of brain structural changes in the WCG (Erickson 2013; Thomas and Baker 2013a, b; Fields 2013).

Materials and methods

Subjects

Thirteen right-handed world class gymnasts (7 F/6 M; 17–24 years; mean ± SD = 20.5 ± 3.3 years) were recruited for this study. All of them have won gold medals in the gymnastic world championships or the Olympic Games since 2007 (Table 1). The gymnasts had started gymnastic training at an average age of 4.5 years and had had more than 12.5 years of training with a mean training time of 6 h/day. We also recruited 13 healthy right-handed subjects as the controls (7 females/6 males; 19–28 years, mean ± SD = 22.5 ± 2.8 years), who were gender- and age-matched with the world class gymnasts. All participants had no history of neurological or psychiatric diseases or brain injuries. The protocols were approved by the Review Board of the Institute of Cognitive Neuroscience and Learning at Beijing Normal University. Informed written consent was obtained from each participant prior to the MR scanning.

Data acquisitions

All images were acquired on a 3T Siemens Trio TIM MR scanner with a 12-channel phased array receive-only head coil. Foam pads and headphones were used to reduce head motion during MRI data acquisition. Diffusion tensor

imaging (DTI) data were obtained using a twice-refocused spin-echo diffusion-weighted echo-planar imaging sequence (Reese et al. 2003). The sequence parameters were as follows: repetition time (TR) = 10,000 ms, echo time (TE) = 92 ms, 64 non-linear directions with $b = 1,000$ s/mm^2 and one volume with $b = 0$, field of view (FOV) = 256 × 248 mm, data matrix = 128 × 124, slice thickness = 2 mm without gap, voxel size = 2 × 2 × 2 mm^3, bandwidth = 1,502 Hz/pixel, k-space coverage 6/8, 75 transverse slices covering the whole brain. Meanwhile, high-resolution (1 mm^3 isotropic) brain structural images were acquired using the 3D T_1-weighted magnetization-prepared rapid gradient echo (MP-RAGE) sequence (TR/TE = 1,900 ms/3.44 ms, inversion time = 900 ms, flip angle = 8°, FOV = 256 × 256 mm, data matrix = 256 × 256, slice thickness = 1 mm, bandwidth = 190 Hz/pixel, and 176 sagittal slices). Both the DTI data and 3D brain structural images were acquired with the Generalized Auto-Calibrating Partially Parallel Acquisitions (GRAPPA) scheme (Griswold et al. 2002) using a GRAPPA factor of 2 and 24 reference lines.

All subjects were scanned on the same scanner in the State Key Laboratory of Cognitive Neuroscience and Learning, Beijing Normal University. For each subject, the DTI and MP-RAGE sequences were repeated three times in the same scanning session to acquire three sets of DTI and three sets of 3D brain structural data in a total scan time of about 50 min. The goal was to investigate the repeatability or reproducibility of the effect size of brain structural changes in world class gymnasts, as derived using VBM, TBSS, and FA-VBA methods. We visually checked all the images on site and found that all showed good image quality.

Data processing

All images were processed using the FSL package version 4.1 (http://www.fmrib.ox.ac.uk/fsl).

T_1-weighted 3D data and VBM analysis of GM density

The VBM analysis was performed according to the standard protocol using FSL-VBM. For each subject, we first extracted the brain data from T_1-weighted 3D images and then performed a tissue-type segmentation to obtain GM, WM, and cerebrospinal fluid (CSF) images. The GM partial volume estimate (PVE) images were aligned to the Montreal Neurological Institute (MNI) standard space using the affine registration tool FLIRT, followed by a non-linear registration using FNIRT. The resulting images were averaged to create a study-specific template at a 2 × 2 × 2 mm^3 resolution in the MNI standard space, to which the native GM images were then non-linearly re-registered. To correct for local expansion or contraction, the registered PVE images were smoothed by a range of isotropic Gaussian kernels ($\sigma = 3$ mm) which is equivalent to a full-width-at-half-maximum (FWHM) of 7 mm. Finally, we applied the general linear model (GLM) with a permutation-based nonparametric testing (5,000 times permutation) to detect the group differences in GM density.

DTI data and tract-based cross-subject analysis of FA in WM

For each DTI dataset, we corrected both the eddy-current induced distortions and the head motions by registering all the images to the b_0 images (the less-distorted T_2-weighted images acquired without diffusion weighting) using an affine registration tool FLIRT. An FA map was calculated by fitting a tensor model to the corrected DTI dataset at each voxel. Then, we carried out voxel-wise analyses of the FA maps across the subjects using the TBSS method. First, the FA maps for all subjects were non-linearly registered onto FSL's standard FA template, the FMRIB-58 FA template, and averaged to generate a study-specific FA map at a 1 × 1 × 1 mm^3 resolution in the MNI standard space. Next, the nearest maximum FA of each registered FA image was projected onto a WM skeleton derived from the FMRIB-58 FA template at a threshold of FA > 0.20. The goal of this projection was to remove any possible residual effect of cross-subject spatial variability after the non-linear registration and to generate a WM tract skeleton that represented the center of the tracts common to all subjects. Then, using a non-linear transform included in FSL, we utilized these FA maps to project local tract centers onto the skeleton for each subject individually. Finally, we applied GLM with a permutation-based nonparametric testing (5,000 times permutation) to detect between-group differences in the FA of the WM.

DTI data and voxel-based cross-subject comparison of FA in GM

In order to estimate the between-group differences in the FA values for the brain GM, we performed a FA-VBA calculation based on the FA images of both the WCG and the controls. Each subject's FA image was warped into the MNI standard space and then voxel-based statistics were carried out to identify clusters where the FA values in the WCG group were different from those of the control group. The calculation procedures were similar to those we used for the VBM.
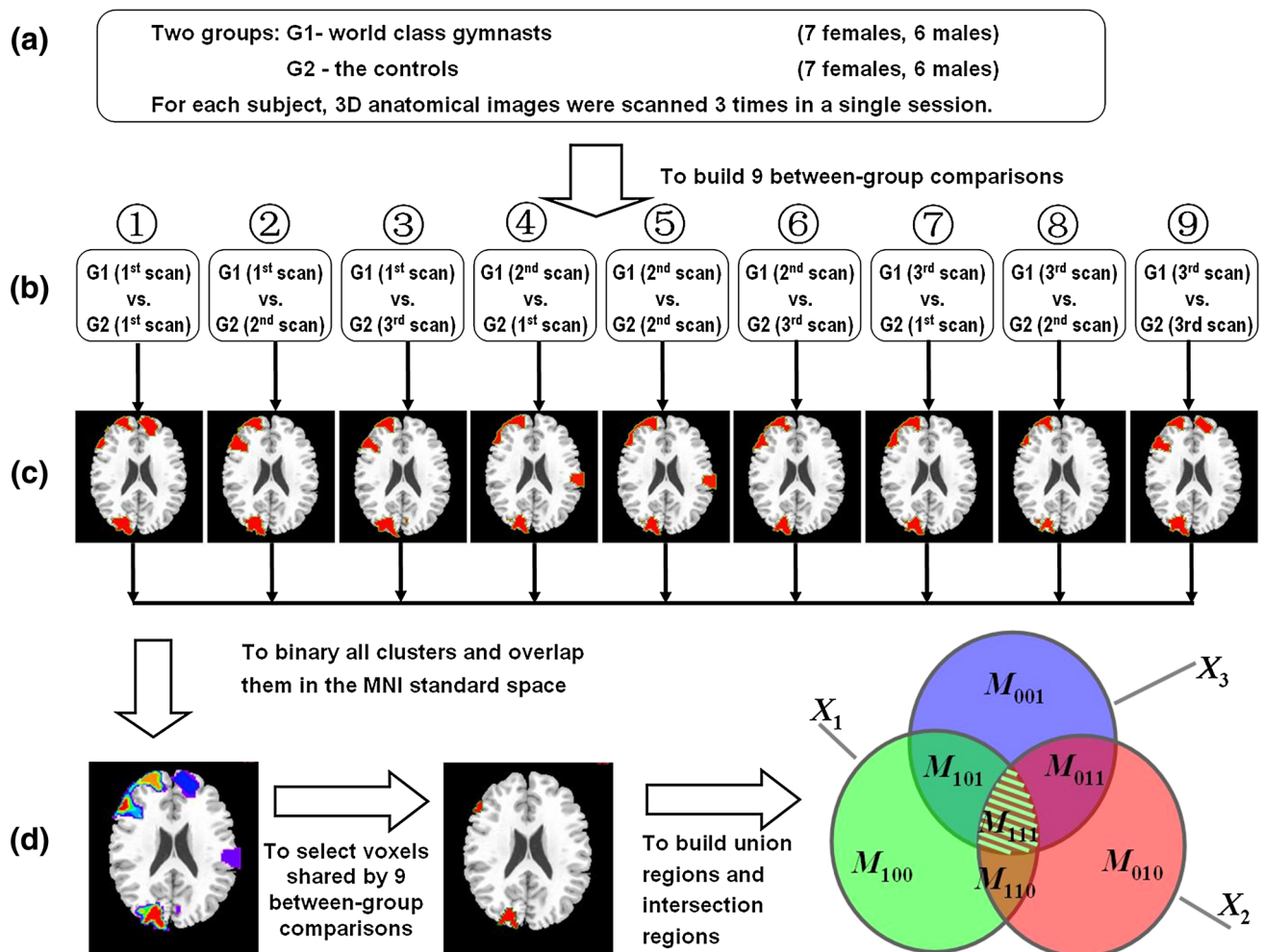
Fig. 1 Schematic for the construction of spatially overlapping regions and intersecting regions using all the between-group comparisons. **a** Each subject was scanned three times to obtain three volumes of 3D high-resolution brain anatomical images in a single session. **b** We constructed nine between-group comparisons based on the three scans of the 3D anatomical images for the WCG and the controls, separately. **c** Statistical analyses detected the ROIs or cluster regions ($p < 0.05$, corrected) that showed differences in brain gray matter density for a between-group comparison. **d** The detected ROIs from each of nine between-group comparisons were binaried and overlapped in MNI standard space. We constructed the union region and the intersecting regions

Statistical analysis

We constructed nine between-group comparisons between the WCG and the controls based on the three repetitive scans of the 3D brain structural images and the three repetitive DTI datasets (Fig. 1). One of our goals was to reduce false-positive findings (Thomas and Baker 2013a, b) in the morphometric estimation by comparing the two subject groups and to pinpoint the size and location of the brain structural changes in the gymnasts. For each between-group comparison, we ran cluster-level statistical comparisons across all subjects for the VBM, TBSS, and FA-VBA analyses using a nonparametric permutation test (Hayasaka et al. 2004). In this procedure, corrections for multiple comparisons were completed using Gaussian random field theory and corrected using a family-wise error rate (FWE) approach (Smith and Nichols 2009). We concluded that the clusters defined at a threshold of $t > 2.3$ and a cluster significance of $p < 0.05$ (FWE-corrected) across all subjects were the brain regions that showed significant between-group differences.

With the aim of reducing false-positive findings about the size and location of brain regions (Thomas and Baker 2013a, b), we first constructed nine between-group comparisons for performing the VBM, TBSS, and FA-VBA analyses. We then generated the intersecting regions and the union regions by overlapping all clusters derived from these nine between-group comparisons in the MNI standard space (Kung et al. 2007; Maitra 2010). Unlike the conventional way of inferring significant difference brain regions based on a single between-group comparison, we used multiple between-group comparisons to construct the

overlapping regions and obtained the intersecting regions across all of the between-group comparisons in this study. This is a more conservative method for reporting effective size and can reduce the effect of false positives. In Fig. 1, we present VBM as an example to illustrate these steps. In step 1, the three 3D brain structural datasets were labeled as the 1st, 2nd, and 3rd scans for the WCG and the matched controls separately (Fig. 1a). We re-grouped these scans and constructed nine between-group comparisons (Fig. 1b). In step 2, we obtained the regions of interest (ROIs) that showed significant structural differences from the VBM analysis for each of the between-group comparisons (Fig. 1c). In step 3, after overlapping all the ROIs derived from these nine between-group comparisons onto MNI-152 standard space, we obtained the overlapping region or the union regions (the voxels that appeared in any of between-group comparisons) and the intersecting regions (Fig. 1d, Fig. S1 in the supplementary materials). In step 4, we determined the size and the center-of-gravity (CoG) of the intersecting regions and reported these as the regions that showed significant difference in brain structure between the WCG and the controls.

Results

Structural changes in GM density

For each between-group comparison, we carried out a VBM analysis on the T_1-weighted structural images and identified the clusters that showed significant between-group differences in brain GM density. Similar procedures were performed, and the cluster regions with altered GM densities were obtained for all nine between-group comparisons (Fig. 1). We created a binary mask, that is, the region-of-interest (ROI) that we used in the study, for each of these clusters and overlapped all the ROIs derived from these nine between-group comparisons in MNI-152 standard space, as shown in Fig. 1 and Fig. S1 in the supplementary materials. Each voxel in the overlapping regions was assigned a value from 1 to 9 to represent the number of between-group comparisons that showed a significant alteration in the GM density in the WCG group for each of these voxels. This means that, for a given voxel in the overlapping regions, if this voxel was found to show a significant alteration in GM density in one of the nine between-group comparisons, we assigned it a value of 1; if this voxel was detected in two of the nine between-group comparisons, we assigned it a value of 2; and so on. We extracted the voxels identified in all nine between-group comparisons and refer to the regions that consisted of these voxels as the intersecting cluster regions (Fig. 1), and reported them in this study. For each of the significantly

increased or decreased ROIs in each of between-group comparisons, we performed the above overlapping steps separately.

We detected three intersecting clusters that had significantly greater GM density ($p < 0.05$, corrected) in the WCG group than in the controls based on the intersections derived from the nine between-group VBM analyses. In Fig. 2, the three intersecting clusters are color-coded in red to provide a three-dimensional visualization (the 2D visualization of the three clusters can be found in Fig. S2 in the supplementary materials). Their sizes and locations are listed in Table 2. The first cluster region (the MNI coordinate of its CoG: $x = -43.9$, $y = 29$, $z = -0.28$) was located in the left inferior frontal gyrus (IFG). The second cluster ($x = -22.2$, $y = -80.3$, $z = 36.9$) was located in the left superior occipital cortex, left inferior parietal lobule (IPL), left superior parietal lobule (SPL), left superior lateral occipital cortex (LOC), left cuneus, and left angular gyrus (AG). The third cluster ($x = 43.7$, $y = -47.3$, $z = 53.1$) was located in the right IPL, right SPL, right superior LOC, right postcentral gyrus (PoCG).

FA changes in the WM

FA maps were used to detect statistically significant differences in the WM structure between the WCG group and the controls. After overlapping the ROIs derived from these nine between-group comparisons, we obtained the WM intersecting regions and found that the values of the FA in the intersecting regions were lower in the WCG group than in the matched controls. Figure 3a–d shows that the locations of the intersecting regions in the two hemispheres were nearly symmetrically distributed. In Table 2, we listed these intersecting regions, which included small parts of the bilateral inferior occipitofrontal fasciculus (IOF), superior longitudinal fasciculus (SLF), inferior longitudinal fasciculus (ILF), posterior thalamic radiation (PTR), anterior thalamic radiation (ATR), and optic radiation (OPR). The detailed locations of the altered WM regions derived from TBSS can also be found in Fig. S3 in the supplementary materials.

We de-projected these intersecting regions back onto each individual FA map to visually verify that the voxels that showed significant effects were indeed located within the WM of each subject. Meanwhile, we calculated the value of the FA for the intersecting regions in each individual FA map. Figure 3e shows the histogram of the FA that corresponds to the WM intersecting regions for each subject and the histograms of the mean FAs for the WCG (in red) and the control groups (in green). This figure indicates that the peak of the FA histogram for the WCG group was skewed to the left with smaller FA values. Figure 3f shows a plot of the mean FA values, sorted from
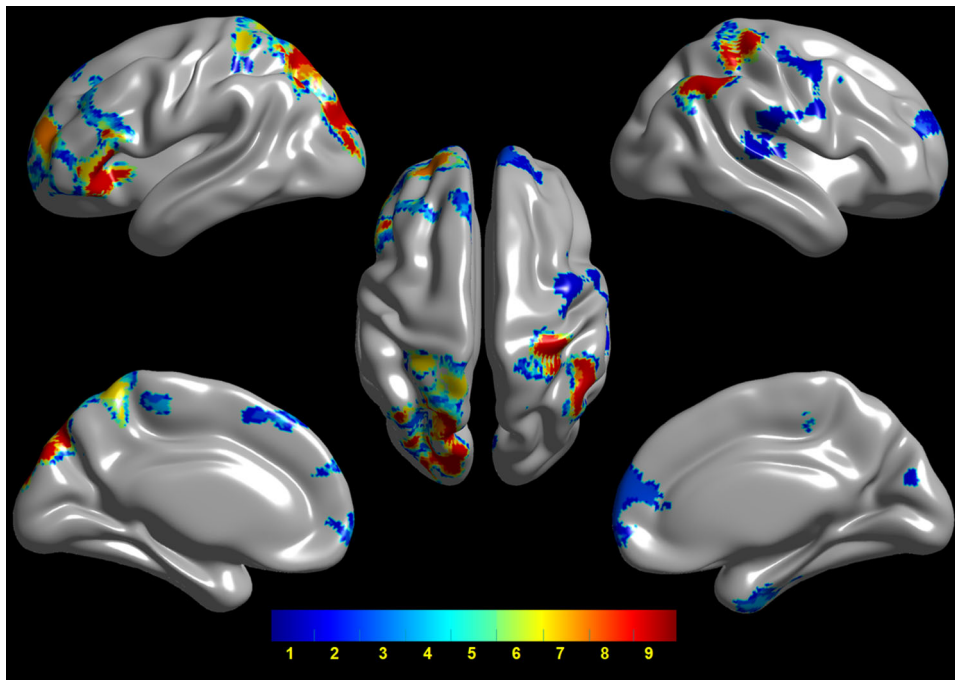
Fig. 2 Changes in the GM density obtained by the VBM method and viewed in different orientations. For each between-group comparison, we binaried the ROIs that showed significant differences in brain GM in the WCG group compared with the controls. After overlapping the binaried ROIs that resulted from all nine between-group comparisons in MNI standard space, we scaled the voxels that appeared in the overlapping regions from 1 to 9 to indicate whether the voxels were detected in 1, 2, . . ., or up to all nine of the between-group comparisons. The *color-bar* indicates the values for each voxel, and the intersecting regions, including the left IFG, bilateral SPL, bilateral IPL, bilateral superior occipital cortex, left cuneus, left angular gyrus, and right PoCG, are color-coded in *red* to represent an increase in GM density in the WCG

lower to higher, of the WM intersecting regions for all subjects. Note that the mean FA values in the WM intersecting region were in the range of 0.55–0.62 for the WCG group and 0.60–0.71 for the matched control group. These findings were well above the typical FA values for GM (FA < 0.25) (Beaulieu 2002; Mori and van Zijl 2002).

FA changes in the GM

To investigate training-induced changes in the GM microstructure, we also tested differences in the FA value of the GM using the FA-VBA method. From all nine between-group comparisons, we obtained the intersecting regions which showed a decreased FA in the GM in the WCG group (Fig. 4). A 2D visualization of the intersecting regions can also be found in Fig. S3 in the supplementary materials. Table 2 lists the intersecting regions, which were located in the left postcentral gyrus and sulcus (primary somatosensory cortex, S1, BA 2L and BA 3L), left supplementary motor area (SMA, BA 6L), bilateral primary motor cortex (M1, BA 4), and bilateral middle cingulate cortex (BA 23).

We de-projected these intersecting regions from the MNI standard space back to each individual diffusion space. The FA values for all the voxels falling in the GM

intersecting regions were calculated for each subject. Figure 4e plots the histogram of the FA values in these intersecting regions for each subject, the mean FA values for the WCG group (in red) and the control group (in green). From this we can see that the FA histogram of the WCG group was lower than that of the controls. The bar plot in Fig. 4f shows the mean FA values of the intersecting region for every subject in the two groups, sorted from low to high FA values. This bar plot indicates that the mean FA of the intersecting regions in the WCG group (in red) was less than that of the controls (in green). This figure also showed that the mean FA values of the intersecting regions were in the range of 0.169–0.206 for the control group and 0.157–0.214 for the WCG group. These values are in the range of the typical FA values for GM (FA < 0.25) (Beaulieu 2002; Mori and van Zijl 2002), indicating that the voxels in the intersecting regions were located in the brain GM.

Discussion

This study seems to support the claim that neuroplasticity can be induced by the acquisition and execution of the complex motor skills involved in long-term intensive

Table 2 The intersecting regions detected using VBM, TBSS, and FA-VBA showing statistically significant differences in brain gray matter and white matter between the world class gymnasts and the controls

Method	Cluster # of voxels (volume in mm^3)	Center of gravity (x, y, z) mm	Location	Anatomical regions
VBM	644 (5,152)	(−43.9, 29, −0.28)	Frontal_Inf_Orb_L	BA 38L, 45L, 47L
			Frontal_Inf_Tri_L	
			Insula_L	
	1,277 (10,216)	(−22.2, −80.3, 36.9)	Lateral occipital cortex (superior division) L	BA 7L, 17L, 18L, 19L, 39L
			Superior parietal lobule L	
			Inferior parietal lobule PGp L	
			Parietal_Inf_L	
			Occipital_Sup_L	
			Occipital_Mid_L	
			Cuneus_L	
			Angular_L	
	1,089 (8,712)	(43.7, −47.3, 53.1)	Lateral occipital cortex (superior division) R	BA 1R, 2R, 3R, 4R, 6R, 7R, 39R, 40R
			Inferior parietal lobule PGp R	
			Inferior parietal lobule PGa R	
			Parietal Lobe	
			Angular_R	
			Parietal_Inf_R	
			Parietal_Sup_R	
			Occ_Mid_R	
			Postcentral_R	
TBSS	In the left hemisphere 251 mm^3	(60.2, −41.1, 15.1)	SLF, ILF, IOF, ACR, PTR, ATR, OPR	
	In the right hemisphere 266 mm^3	(35.5, −35.2, 5.4)	SLF, ILF, IOF, ACR, PTR, ATR, OPR	
FA-VBA	914 (7,312)	(−5.53, −29.1, 46.6)	Cingulum_Mid_L	BA 2L, 3L, 4L, 4R, 6L, 23L, 23R
			Cingulum_Mid_R	
			Parietal_Sup_L	
			Postcentral gyrus L	
			Postcentral sulcus L	
			Superior parietal lobule L	
			Postcentral lobule L/R	
			Supplementary motor area L/R	
	27 (216)	(−12.7, −14.4, 53.7)	Supplementary motor area L	BA 6L

JHU-ICBM-DTI-81 White Matter Labels and JHU-White Matter Tractography Atlas were used to label the white matter structure (Oishi et al. 2008)

CoG center-of-gravity in MNI space, *L (R)* the left (right) hemisphere, *SLF* superior longitudinal fasciculus, *ILF* inferior longitudinal fasciculus, *IOF* inferior occipitofrontal fascicle, *ACR* acoustic radiation, *PTR* posterior thalamic radiation, *ATR* posterior thalamic radiation, *CT* corticospinal tract, *rIC* retrolenticular part of the internal capsule, *SS* sagittal stratum (include ILF and IOF)

gymnastic training and that this functional neuroplasticity is accompanied by structural changes in both the GM and WM (Pascual-Leone et al. 2005; Buonomano and Merzenich 1998). We found a local reduction in the FA of the WM along with a local increase in GM density in the WCG group compared with the control group. Our findings were confirmed by using the intersecting regions, which were exactly the same in all nine between-group comparisons.

Structural changes in the GM of the WCG group

Adaptive brain structural changes are essential for effective participation in high-performance sports. Using the VBM analysis, we detected a local increase in GM density in three clusters in the brains of the world class gymnasts (Fig. 2; Table 2, and Figs. S1–S2 in the supplementary materials). The first cluster was located in the left IFG,
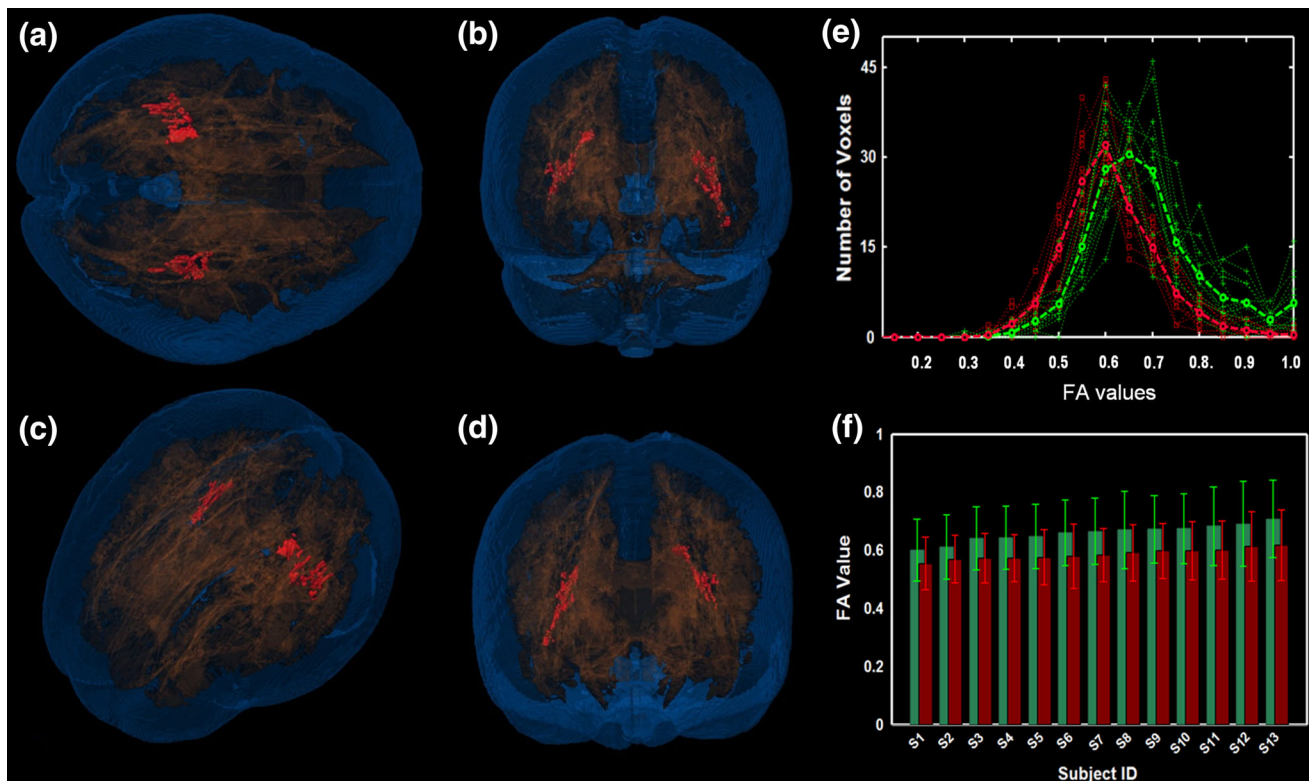
Fig. 3 TBSS detected the intersecting regions in the WM, including the bilateral SLF, ILF, and IOF, that showed a decrease in the fractional anisotropy (FA) value in the WCG. The intersecting regions are color-coded in *red*. The centers-of-gravity were (60.2, −41.1, 15.1) mm and (35.5, −35.2, 5.4) mm in MNI standard space, and their corresponding sizes were 251 and 266 mm^3, respectively, for the altered FAs in the WM tracts in the left hemisphere and the right hemispheres. The brain is visualized in the (*a*) superior, (*b*) backward, (*c*) right lateral, and (*d*) frontal orientations. (*e*) The *dotted lines* show the histogram of the FAs for each subject and the *dashed thick lines* show the average histogram of the FA across each group in the intersecting region. (*f*) The *bar plots* show the mean FAs of all the voxels for each subject (S1, S2,...,S13). The mean FA was sorted from lower to higher values for all subjects. *Error bars* represent standard deviations. *Bars* and *lines* are color-coded in *red* and *green* to represent the WCG and the controls, respectively. The mean FAs were in the range of 0.55–0.62 for the WCG group, and 0.60–0.71 for the matched control group. Both sets of values were well above the typical FA values for brain gray matter (FA < 0.25)

which is associated with the inhibitory control of motor responses (Swick et al. 2008) and with contextual control in which external contextual signals are used to select between various premotor representations (Koechlin et al. 2003). The second cluster included the left IPL and left SPL, left superior LOC, left cuneus, and left AG (Table 2). The left parietal lobule (PL) is a highly heterogeneous region. Previous studies indicated that the left PL is involved in visuospatial attention, memory, mathematical cognition (Uddin et al. 2010), intention to perform specific motor acts (Colby and Goldberg 1999), and planning movements (Andersen et al. 1997). The left IPL, which showed signficant changes in GM density in the champions, is also believed to be involved in mental arithmetic accompanied by memory and attentional resources (Rivera et al. 2005), integrating time and space during collision judgments (Assmus et al. 2003), integrating internal information about the body, and processing external information about an object (Naito and Ehrsson 2006). The

SPL is similarly believed to be involved in motion perception (Vaina et al. 2001), mental rotation tasks (Jordan et al. 2002), and bimanual movements (Wenderoth et al. 2004). The LOC plays an important role in human object recognition and selection (Grill-Spector et al. 2001). Previous studies indicated that the LOC is a specialized region for distinguishing items within a category (Welberg 2012), processing multiple within-scene objects (Peelen and Kastner 2011; MacEvoy and Epstein 2011), and representing both simple image features and higher level shape information (Kourtzi and Kanwisher 2001; Vinberg and Grill-Spector 2008). The changes that we found in GM density in the left superior LOC may indicate that the champions have a fast and accurate recognition of both the identities and positions of objects in visual space (MacEvoy 2013). The left cuneus is known for its involvement in basic visual processing. Previous studies indicated that the cuneus is involved in the bottom–up control of visuospatial selective attention called stimulus-driven attention (Hahn
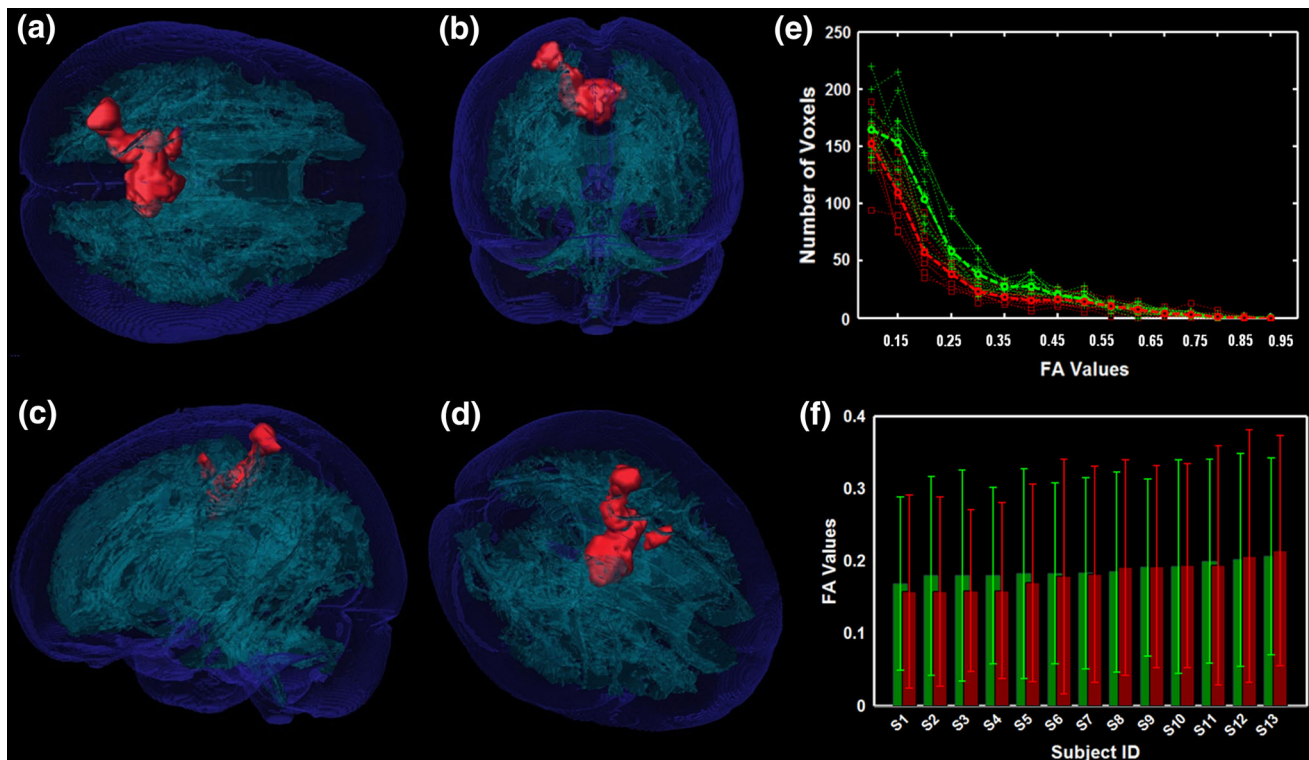
Fig. 4 FA-VBA detected intersecting regions that showed a decreased fractional anisotropy (FA) value in the brain GM of the WCG. Voxels included in the intersecting regions are color-coded in *red*. The brain was viewed in (*a*) superior, (*b*) backward, (*c*) right lateral, and (*d*) frontal orientation. (*e*) *Dotted lines* relate to the histogram of FAs for each subject and the *dashed thick lines* to the average histogram of the FA across each group in the intersecting region. (*f*) *Bar plots* show the mean FAs of all voxels for each subject (S1, S2, ..., S13). The mean FA was sorted from lower to higher values for all subjects. *Error bars* represent standard deviations. *Bars* and *lines* are color-coded in *red* and *green* to represent the WCG and the controls, respectively. The averaged FA values across all voxels in the intersecting regions for each control subject were in the range of 0.17–0.21 and of 0.16–0.21 for each champion, values which are in the range of typical FA values of brain GM (FA < 0.25)

et al. 2006), and is also interconnected with the default mode network and limbic regions for vigilance, attention, motivation, and arousal (Breckel et al. 2011). The AG plays a major role in retrieving information held in the memory system of the brain. Grabner et al. (2009, 2013) and Ansari (2008) indicated that the left AG can mediate the automatic mapping of arithmetic problems onto solutions stored in memory. Seghier et al. (2010) segregated the left AG into three different sub-regions and suggested different sub-region responds to goal-directed tasks in different ways. The left middle AG is involved in semantic associations regardless of the presence or absence of a stimulus, the left dorsomesial AG involved in searching for semantics in all visual stimuli, and the left ventrolateral AG involved in the conceptual identification of visual inputs. The third cluster was located in the right SPL, the right IPL, right SPL, right superior LOC, and right PoCG (S1 or primary somatosensory cortex). The right PoCG receives information primarily from the skin and muscles, allowing the experiences of touching, reaching, and grasping (Iwamura and Tanaka 1996). Previous studies suggested that the PoCG is involved in the processing and mediating

of tactile information (Song and Francis 2013) and skilled motor learning (Vidoni et al. 2010). The functions of the right SPL, the right IPL, right SPL, and right superior LOC are similar to those of the corresponding left regions. Taking all these findings into consideration, we speculate that, as a result of their routine gymnastic practice, the gymnastic champions possess an extraordinary ability to estimate the direction of movements, the speed of execution, and the identification of their own and surrounding objects' locations.

In this study, using the FA-VBA method, we detected FA changes in the left SMA (BA 6L), bilateral primary motor cortex or M1 (BA 4), left postcentral gyrus and sulcus (primary somatosensory cortex or S1, BA 2L and 3L), and bilateral middle cingulate cortex (BA23) in the champions compared with the controls (Fig. 4 and Fig. S3 in the supplementary materials). The FA values in these regions were uniformly lower in the champions than in the controls (Fig. 4). The SMA is considered to play an important role in the temporal organization of movements and contains a somatotropic representation of the body (Goldberg 1985; Nachev et al. 2008), just like the primary

motor cortex (Tanji 1996, 2001). Previous studies have suggested that the SMA controls postural stability during standing or walking (Penfield and Welch 1951), coordination of temporal sequences of actions (Tanji 1994; Shima and Tanji 1998; Roland et al. 1980; Lee and Quessy 2003), and bimanual coordination (Brinkman 1981). The primary motor cortex, or M1, is one of the principal brain areas involved in motor function and is considered the main generator of the neural impulses that pass down to the spinal cord to control the execution of movement. Evarts (1968) suggested that each neuron in the motor cortex contributes to the force of a muscle. The greater the number of neurons that are activated in the motor cortex, the greater the muscle force. Georgopoulos et al. (1986, 2007) trained monkeys to reach in various directions while he monitored the activity of neurons in the motor cortex and found that each neuron in the motor cortex was maximally active during a specific direction of reach and responded less well to neighboring directions of reach. Other studies revealed that the M1 is essential to the early stage of motor consolidation (Muellbacher et al. 2002) and to the precise execution of learned motor responses (Hasan et al. 2013). Several studies also suggested that both the SMA and M1 play an important role in the execution of complex sequential finger movements (Shibasaki et al. 1993), motor control and motor skills (Ward et al. 2006), and multisensory representation (Lloyd et al. 2003). The roles of the primary somatosensory cortex or S1 (BA 2 and 3) include the processing and mediating of tactile information (Song and Francis 2013) and skilled motor learning (Vidoni et al. 2010). The cingulate cortex (BA 23) is also involved in mental (Tanaka et al. 2005), attentional and executive processing (van Veen et al. 2001), and in decision making (Bush et al. 2002; Kennerley et al. 2006). Thus our results may reflect the effects of the long-term intensive professional training on the brain plasticity of gymnasts. Our findings may indicate that professional gymnasts, especially gymnastic world champions, not only possess good motor or motion abilities, including physical strength, power, coordination, and agility, but also very good judgment and decision making ability. We also noticed that the regions (BA 2L, 3L, and 6L) that showed significant FA changes were lateralized to the left hemisphere, which may reflect the effect of right handedness in the gymnasts that participated in this study on brain plasticity (Amunts et al. 2000).

That reduced FA values in the GM observed in the gymnasts may indirectly reflect the microstructure changes as a result of the long-term gymnastic training. FA is an index to characterize tissue microstructure, and its values are vastly different in different GM and WM regions (Basser and Pierpaoli 1996; Pierpaoli and Basser 1996). As a major component of the central nervous system, GM also has complex microstructures, consisting of neuronal cell bodies, dendrites, unmyelinated axons, glial cells, synapses, and capillaries. Cellular changes in any of these may influence the MRI signal or the FA value. Because the DTI technique only detects signals from water molecules, it is not usually possible to infer correspondence between changes in the MRI signal (or FA value) and a specific under-lying biological event. Therefore, mapping the FA in the brain GM may only indicate the degree of complexity of the cortical anatomy, and such FA alterations should only be considered to be an indirect parameter that may reflect critical changes of brain tissue microstructures. Whether structural MRI and DTI can measure cellular events even though they give rise to a global quantity still remains poorly understood (Zatorre et al. 2012), and a direct link between micro-structures and macrostructures has not been established for the human brain.

Taken together, finding that those specific regions in the WCG had a local increase in GM density and a local decrease in FA in the GM may indicate that the gymnasts' long-term intensive training induced significant brain structural changes as a result of motor skill acquisition and development. These changes may be associated with reductions in reaction time and increments in accuracy that result from the repeated performance of serial motor tasks in gymnastic training.

Structural changes in the WM of the WCG group

A gymnast requires complex visuo-motor integration of reaching, jumping, and grasping movements. The present study detected local reductions in the FA in parts of the bilateral SLFs, ILFs, and IOFs of the WCG group compared with the controls (Fig. 3; Table 2, and Fig. S3 in the supplementary materials). The fronto-parietal network plays a key role in the coordination and planning of complex motor skills (Coull et al. 1996; Rizzolatti and Luppino 2001). The SLF is associated with the dorsal visual stream and connects the frontal, occipital, parietal, and temporal lobes, connections which are crucial for the visual localization of objects. The ILF, however, is associated with the ventral visual stream and connects the occipital and temporal lobes, connections which are crucial for object identification (Hoeft et al. 2007). The motor responses are mediated by both pathways in gymnastic training. Moreover, the IOF originates from dorsal parieto-occipital and medial parietal areas and projects into lateral prefrontal areas (Rizzolatti et al. 1983), a location which may influence visual-spatial processing within the occipital and parietal areas through the IOF. A previous study (Schmahmann et al. 2007) suggested that the IOF may be related to higher-order aspects of motor behavior and to spatial aspects of attention. Another study (Oechslin et al.

Table 3 Brain regions showing significant changes in brain GM density in the trained subject group compared with the control group using the VBM method

Subjects and age	Trained period	GM density in trainers	Location	(x, y, z) mm	Cluster size (mm³) or # of voxel (voxel size = 2^3 mm³)	References
Taxi drivers						
16 Drivers, 50 controls Age: 32–62, mean = 44	Driving age 1.5–42 years Mean = 14.3 years	↑	Posterior Hippocampi_L&R	(−31, −28, −10) (31, −22, −13)	75 mm³ 77 mm³	Maguire et al. (2000)
Musician (Symphony Orchestra)						
26 Musicians (age 43.2 ± 9.3 years); 26 Controls (age 42.8 ± 10.8 years)	20.4 ± 9.4 years	↑	IF_L	(−46, 18, 3)	699 mm³	Sluming et al. (2002)
Pianists						
Professional 20 (age 23.05 ± 3.83 years); Amateur 20 (age 25.95 ± 5.61 years); Nonmusician 40 (age 26.92 ± 4.90 years)	6.00 ± 1.81 years 7.65 ± 4.17 years	↑	IT_L, R; Precentral_L, R SP_R, MedF_R; Heschl's_L; Larsell lobes HV, HVI			Gaser and Schlaug (2003)
Jugglers						
12 Trained, 12 control; (age 22 ± 1.6 years)	3 months	↑	hMT V5 bilateral, PIP_L	(−43, −75, −2) (33, −82, −4) (−40, −66, 43)		Draganski et al. (2004)
Second language learners						
33 'Late' bilinguals, 25 'Early' bilinguals 25 Monolinguals;	10–15 years	↑	IP_L&R	(−45, −59, 48) (56, −53, 42)		Mechelli et al. (2004)
Mathematicians						
26 Mathematicians (age 35.50 ± 6.95); 23 Controls (age 35.43 ± 7.62 years)	16.1 ± 3.3 years	↑	IPL_R IPL_L IF_L	(54, −58, 38) (32, −46, 60) (57, −60, 34) (−38, −50, 57) (−42, −34, 12)		Aydin et al. (2007)
Jugglers						
24 Trained, 24 controls;	6 weeks	↑	Medial occipital, parietal lobe	(−10, −70, 36)	500 voxels	Scholz et al. (2009)

Table 3 continued

Subjects and age	Trained period	GM density in trainers	Location	(x, y, z) mm	Cluster size (mm³) or # of voxel (voxel size = 2³ mm³)	References
Ballet dancers						
10 Dancers, 10 controls; (age 35.8 ± 7.8 years)	14.2 ± 3.3 years	↓	GM: PM_L	(−7, 18, 62)	3,063 voxels	Hänggi et al. (2010)
			Putamen_L	(−22, 8, −5)	5,177 voxels	
			SMA_L&R	(−6, −2 46), (1, 9, 38)	2,161 voxels	
			SFG_L	(−13, 28, 45)	3,224 voxels	
Golfers						
10 Professionals (age 30.9 ± 6.2 years)	Year of start/ training	↑	PIP_L	(−46, −67, 39)	171 voxels	Jäncke et al. (2009b)
10 High skilled (age 26.6 ± 8.3 years)	13.1 ± 5.6/ 17.8 ± 9.4 years		PPC_L	(−18, −69, 52)	62 voxels	
10 Intermediate (age 26.5 ± 8.4 years)	14.5 ± 8.4/ 12.1 ± 3.5 years		dPM_R	(22, 22, 63)	137 voxels	
10 Controls (age 25.9 ± 2.0 years)	19.0 ± 7.2/ 7.6 ± 6.0 years n.a./n.a.		cPM_L	(−52, 23, 56)	50 voxels	
World class gymnasts						
13 Champions, 13 controls; (age 20.5 ± 3.3 years for champions, 20.3 ± 2.5 years for controls)	16.1 ± 3.3 years (6 h/day)	↑	See Table 2	(−22.2, −80.3, 36.9)	1,277 voxels	Current study
				(43.7, −47.3, 53.1)	1,089 voxels	
				(−43.9, 29, −0.28)	644 voxels	

Table 4 Brain regions showing significant changes in fractional anisotropy (FA) in brain white matter and gray matter in the trained subject group compared with the control group using TBSS and FA-VBA methods

Subjects and age	Trained period	FA changes in trainers	Location	(x, y, z) mm	Cluster size (mm³)	References
Pianists	Childhood 1,618 ± 662 h;	↑	PIC_R, Splenium	(27, −20, −36)	1,322	Bengtsson et al. (2005)
8 Musicians (males)	Adolescent: 3,195 ± 1,515 h		And body of CC,	(31, −67, 24)	1,257	
8 Controls (males) (age 32.6 ± 5.7 years)	Adulthood: 22,971 ± 9,413 h		AIC_L, IC	(13, −7, 32)	1,024	
	5.8 years ± 1.4 (age of start)		Arcuate fasciculus	(−16, 7, 12)	415	
Jugglers	6 weeks	↑	PIP_R	(31, −59, 31)	500	Scholz et al. (2009)
24 Trainers, 24 controls						
Pianists	30 months	↑	Middle third of the anterior body of CC	–	–	Schlaug et al. (2009)
18 Trainers, 13 controls; (age 6.49 years)	(1–2 or 2–5 h/week)					
Ballet dancers	14.2 ± 3.3 years	→	PM_L&R	(−28, 7, 42)	4,771	Hänggi et al. (2010)
10 Dancers (35.8 ± 7.8)			MFG_L	(20, 16, 50)	8,417	
10 Age-matched controls			FO	(−31, 29, 29)	3,119	
				(36, 24, 13)	3,140	
Golfers	Year of start/training	→	CST_L	(−14, 26, 28)	875	Jäncke et al. (2009b)
10 Professionals (30.9 ± 6.2 years)	13.1 ± 5.6/17.8 ± 9.4 years		posterior limb. IC	(−6, −27, −18)	126	
10 High skilled (26.6 ± 8.3 years)	14.5 ± 8.4/12.1 ± 3.5 years		IC_R	(35, −35, 8)	383	
10 Intermediate (26.5 ± 8.4 years)	19.0 ± 7.2/7.6 ± 6.0 years		CC	(−33, −38, 6)	309	
1,010 Controls (25.9 ± 2.0 years)	n.a./n.a.		SMA_R	(24, 6, 17)	90	
			SFG_L	(−15, 32, −9)	1,739	
				(14, 0, 40)	208	
				(−16, 28, 47)	53	
Musicians	12.2 ± 3.2 years (age of start)	↑	IF_L	(−30, 31, −9)	497	Han et al. (2009)
19 Pianists (22.6 ± 2.6 years)	10.4 ± 4.2 years (years of training)		PIC_R	(−12, −7, 5)	285	
21 Controls (22.4 ± 2.6 years)			MB_R	(11, −23, −8)	132	

Table 4 continued

Subjects and age	Trained period	FA changes in trainers	Location	(x, y, z) mm	Cluster size (mm³)	References
Musicians 5 Adult subjects with musical training since early childhood 7 Adult controls.(FA-VBA)	–	↑ ↓	genu of the CC Corona radiata and the internal capsule bilaterally	– –	– –	Schmithorst and Wilke (2002)
World class gymnasts 13 Champions, 13 controls; (age 20.5 ± 3.3 years for champions 20.3 ± 2.5 years for controls)	16.1 ± 3.3 years (6 h/day)	↓	See Table 2	(60.2, −41.1, 15.1) (35.5, −35.2, 5.4)	251 266	Current study

AC anterior cingulate, AIP anterior intraparietal sulcus, AIC anterior limb of internal capsule, ATR anterior thalamic radiation, CC corpus callosum, CST corticospinal tract, cPM caudal premotor cortex, dPM dorsal premotor cortex, EC external capsule, FO frontal operculum, MB midbrain, hMT mid-temporal area, IC internal capsule, IF inferior frontal gyrus, IT inferior temporal gyrus, IOF inferior occipitofrontal fascicle, MedF medial frontal gyrus, MFG middle frontal gyrus, PC posterior cingulate, PIP posterior intraparietal sulcus, PIC posterior internal capsule, PPC posterior parietal cortex, PM premotor, SMA supplementary motor area, SFG superior frontal gyrus, SP superior parietal cortex

2009) showed that these regions (the SLF, ILF, and IOF) are related to visual-motor processing and attention control.

Furthermore, we found decreased FA values in certain bilateral projection fibers, including the PTR, ATR, ACR, OPR, and callosal body in the GWC (Table 2). Thalamic radiations, including the PTR and ATR, are the fibers which reciprocally connect the thalamus and cerebral cortex by way of the internal capsule. The ATR passes through the anterior limb of the internal capsule and carries fibers from the hypothalamus and limbic structures to the frontal lobe. The PTR includes the optic radiation from the lateral geniculate body to the primary visual cortex in the occipital lobe. The ACR and OPR are the fibers arising from the thalamus to the primary auditory and occipital cortices. Those projection fibers may be involved in changes in visual and auditory information processing resulting from long-term gymnastic training. In addition, we detected FA changes in the WM in the left rIC, SS, and CT. Finding these changes in only the left side may indicate that these right-handed gymnasts are left-hemisphere dominant and that the storage of the visuo-motor skills involved in long-term intensive gymnastic training is handedness responsive.

Gymnastics, like many sports, requires physical training that builds the overall fitness of the athlete and includes elements of strength, power, speed, endurance, balance, and flexibility. Changes in the WM in these regions could help enable world class gymnasts to be more accurate, efficient, consistent, and automatic in their performances. Our findings were consistent with those of Hänggi et al. (2010) and Jäncke et al. (2009b), in which they revealed a decreased FA in the brain WM of professional ballet dancers and skilled golfers. However, we also found studies of musicians and jugglers that showed an increase in the FA of the WM and that explained those findings as resulting from an increase in the myelination of the WM after training (Gaser and Schlaug 2003; Yarrow et al. 2009; Scholz et al. 2009; Zalc and Douglas Fields 2000). Professional gymnastic training may be different from music practice. Gymnastic practice could be associated either with general WM maturation or with specific, localized WM changes due to the acquisition of a particular skill. In fact, increased FA in WM could be caused by decreased radial diffusion, increased axial diffusion, or a mix of both (Zatorre et al. 2012). Both fiber diameter and WM density are important factors for determining diffusion properties such as FA (Fieremans et al. 2008, 2009). Previous phantom experiments found that fiber bundles with a larger diameter have a lower FA (Fieremans et al. 2008, 2009), and vice versa. Takahashi et al. (2002) measured the FA of lamprey spinal cord WM and discovered that the degree of anisotropy, or the ratio of axial to radial diffusion, decreased from 7.0 (equivalent to FA = 0.82) to 4.2

(FA = 0.69) to 1.9 (FA = 0.34) for the dorsal, dorsolateral, and ventral portions, respectively, with an increase in the mean axon diameter. Therefore, we think it is reasonable to conclude that the gymnasts' long-term intensive training and the acquisition of their motor skills caused an increase in the fiber diameter, which resulted in a decreased FA in the world class gymnasts.

Comparisons with previous studies

We also compared our findings with previous studies of trained groups. Tables 3 and 4 list the size and location of the cluster regions detected in these other studies that used VBM, TBSS, and FA-VBM methods (Hänggi et al. 2010; Maguire et al. 2000; Sluming et al. 2002; Gaser and Schlaug 2003; Draganski et al. 2004; Mechelli et al. 2004; Scholz et al. 2009; Jäncke et al. 2009b; Aydin et al. 2007). Table 3 shows the widely distributed locations and sizes of the detected regions across the brain GM in various training groups. Our study detected a local increase in GM density in the WCG, a finding which was consistent with these previous studies.

We found a local decrease in the FA of both the GM and the WM in the WCG group compared with the control group. These changes may relate to the fact that, after gymnasts practice several hours a day for a number of years, they seem to be able to coordinate and execute their routines effortlessly. These focal GM and WM changes in the WCG group are likely to be the result of intensive and specific training. In Table 4 we noticed mixed findings about the direction of FA changes in the different training groups (Scholz et al. 2009; Bengtsson et al. 2005; Hänggi et al. 2010; Schmithorst and Wilke 2002; Han et al. 2009; Jäncke et al. 2009a; Schlaug et al. 2009). The findings in Table 4 may indicate differential responses to specific behavioral training (Draganski et al. 2004; Scholz et al. 2009; Gaser and Schlaug 2003; Hänggi et al. 2010; Jäncke et al. 2009b; Maguire et al. 2000; Sluming et al. 2002; Mechelli et al. 2004; Aydin et al. 2007; Cannonieri et al. 2007). Possible explanations for these inconsistent results, in which the FA sometimes increased and sometimes decreased in the different training groups, are manifold and need to be further investigated.

Intersecting regions reduce the false-positive discovery rate

Repeatability and reproducibility are crucial for neuroimaging studies (Bennett and Miller 2010). Because no absolute standards are available to validate the output of VBM, TBSS, and FA-VBA calculations, we cannot be sure of the repeatability or reproducibility of the results of the test and retest scans after we complete the voxel-based

statistical comparisons. The ideal situation occurs when the size and location of the cluster regions remain constant regardless of the number of measurements (Thomas and Baker 2013a, b; Bartlett and Frost 2008). However, most studies that have used VBM, TBSS, and FA-VBA methods have not investigated repeatability or reproducibility (Scarpazza et al. 2013). For the first time, to the best of our knowledge, we constructed overlapping regions and intersecting regions using multiple between-group comparisons for reporting the size and location of brain structural changes. This increases the validity of our findings by greatly reducing the false-positive discovery rates (Erickson 2013; Thomas and Baker 2013a, b; Fields 2013; Draganski and Kherif 2013; May and Gaser 2012).

To reduce false-positive findings, researchers can perform several repetitive scans of the brain structural images and construct the intersecting regions from multiple between-group comparisons. In this study, although acquiring three repetitive datasets at one scanning session had the disadvantage of making the participants experience a longer scanning time, it enabled us to pinpoint specific neuroanatomical features in the WCG and to show that common brain regions appeared when using multiple between-group comparisons. This could partially answer the question raised by Thomas and Barker (Thomas and Baker 2013a, b) as to whether the same brain regions would be detected using different measurement methods.

Limitations

The present study has some limitations. First, the biological interpretation in this study is not straightforward and unequivocal. DTI provides a means for investigating changes in the integrity of brain WM but does not make it possible to differentiate the contributions of myelination, fiber diameter and density, and tissue organization to the FA value in brain GM and WM. All these factors influence the distribution of the DTI signal (Beaulieu 2002). No one-to-one relationship can be identified between a particular measure (e.g. FA) and a given brain microstructure. Thus, a variation in any one of these factors might, if large enough, produce an observable effect in the diffusion measures (Fieremans et al. 2008, 2009; Takahashi et al. 2002). As yet, no direct link between micro-structures and macro-structures has been established for the human brain. Second, we only selected a non-linear registration method provided in the FSL to perform the brain normalization. We did not compare the influence of different registration methods on the calculation result. The non-linear registration could potentially affect the spatial normalization of the brain and then confound the between-group comparisons (Klein et al. 2009, Zalesky 2011, de Groot et al. 2013, Radua et al. 2013). Third, we labeled the brain regions

using macroscopic brain templates. This is a rather coarse anatomical labeling method compared with cytoarchitectonic probabilistic maps (Amunts 2013, Eickhoff et al. 2005, Zilles and Amunts 2010, Amunts et al. 2007, 2013). However, because one of our goals was to use the gymnastic champions sample to clarify the advantage of using multiple between-group comparisons in brain structure studies, we were roughly able to label the changed brain regions using the macroscopic brain templates and use these to explain our findings to a certain, but somewhat limited, extent. Fourth, the geometric distortion and diffusion gradients (bvecs or B-matrix) caused by B_0 inhomogeneity and eddy currents, which are problems for diffusion-weighted images (Rohde et al. 2004; Leemans and Jones 2009), were not estimated when processing the DTI data in this study. One reason was that we did not acquire field mapping images for correcting the geometric distortion of the DTI dataset. The other reason was that we thought that the B-matrix effect induced by the head motion would be small in comparison with the signal dropout effects (caused by the field inhomogeneity) that we could not correct for, and we observed that the subjects in this study did not have a significant amount of head motion during the DTI acquisition. Last, but not least, we recruited 13 world champion gymnasts, but we did not perform a longitudinal study to detect the brain structural changes in these gymnasts. Therefore, we cannot completely rule out the possibility that maturation and/or innate predisposition could have caused or contributed to the differences between the WCG and the controls.

Conclusions

Our findings provide new insights into the brain structure changes induced by long-term intensive gymnastic training. To infer the regions with significant differences between the two groups, we introduced, for the first time, intersecting regions derived from multiple between-group comparisons. The results seem to indicate that world class gymnasts possess good motor or motion abilities and good judgment and decision making ability as well as good visuomotor and visuospatial abilities as a result of routine gymnastic practice, and that long-term intensive training may cause an increase in fiber diameter as revealed by the decrease in the FA in WM in the WCG group, as a result of the acquisition of specific motor skills. A better understanding of the changes in GM and WM structure in world class gymnasts will help us to further understand the neural basis of motor skill acquisition and development in elite athletes.

Conflict of interest The authors declare that they have no competing financial interests.

References

Amunts K (2013) Microstructural maps at multiple scales? JuBrain atlas and BigBrain. Frontiers in Neuroinformatics

Amunts K, Jäncke L, Mohlberg H, Steinmetz H, Zilles K (2000) Interhemispheric asymmetry of the human motor cortex related to handedness and gender. Neuropsychologia 38(3):304–312

Amunts K, Schleicher A, Zilles K (2007) Cytoarchitecture of the cerebral cortex–more than localization. Neuroimage 37(4):1061–1065 discussion 1066–1068

Amunts K, Lepage C, Borgeat L, Mohlberg H, Dickscheid T, Rousseau ME, Bludau S, Bazin PL, Lewis LB, Oros-Peusquens AM, Shah NJ, Lippert T, Zilles K, Evans AC (2013) BigBrain: an ultrahigh-resolution 3D human brain model. Science 340(6139):1472–1475

Andersen RA, Snyder LH, Bradley DC, Xing J (1997) Multimodal representation of space in the posterior parietal cortex and its use in planning movements. Annu Rev Neurosci 20:303–330

Ansari D (2008) Effects of development and enculturation on number representation in the brain. Nat Rev Neurosci 9(4):278–291

Ashburner J, Friston KJ (2000) Voxel-based morphometry—the methods. NeuroImage 11(6):805–821

Assmus A, Marshall JC, Ritzl A, Noth J, Zilles K, Fink GR (2003) Left inferior parietal cortex integrates time and space during collision judgments. NeuroImage 20(Suppl 1):S82–S88

Aydin K, Ucar A, Oguz KK, Okur OO, Agayev A, Unal Z, Yilmaz S, Ozturk C (2007) Increased gray matter density in the parietal cortex of mathematicians: a voxel-based morphometry study. AJNR Am J Neuroradiol 28(10):1859–1864

Bartlett JW, Frost C (2008) Reliability, repeatability and reproducibility: analysis of measurement errors in continuous variables. Ultrasound Obstet Gynecol 31(4):466–475

Basser PJ, Pierpaoli C (1996) Microstructural and physiological features of tissues elucidated by quantitative-diffusion-tensor MRI. J Magn Reson B 111(3):209–219

Beaulieu C (2002) The basis of anisotropic water diffusion in the nervous system-a technical review. NMR Biomed 15(7–8):435–455

Benedetta B, Zhaleh K, Mara C, David HM, Alan JT, Olga C (2009) Exploring the relationship between white matter and gray matter damage in early primary progressive multiple sclerosis: an in vivo study with TBSS and VBM. Hum Brain Mapp 30(9):2852–2861

Bengtsson SL, Nagy Z, Skare S, Forsman L, Forssberg H, Ullen F (2005) Extensive piano practicing has regionally specific effects on white matter development. Nat Neurosci 8(9):1148–1150

Bennett CM, Miller MB (2010) How reliable are the results from functional magnetic resonance imaging? Ann N Y Acad Sci 1191:133–155

Breckel TPK, Giessing C, Thiel CM (2011) Impact of brain networks involved in vigilance on processing irrelevant visual motion. NeuroImage 55(4):1754–1762

Brinkman C (1981) Lesions in supplementary motor area interfere with a monkey's performance of a bimanual coordination task. Neurosci Lett 27(3):267–270

Buonomano DV, Merzenich MM (1998) Cortical plasticity: from synapses to maps. Ann Rev Neurosci 21(1):149–186

Bush G, Vogt BA, Holmes J, Dale AM, Greve D, Jenike MA, Rosen BR (2002) Dorsal anterior cingulate cortex: a role in reward-based decision making. Proc Natl Acad Sci USA 99(1):523–528

Cannonieri GC, Bonilha L, Fernandes PT, Cendes F, Li LM (2007) Practice and perfect: length of training and structural brain changes in experienced typists. NeuroReport 18(10):1063–1066

Colby CL, Goldberg ME (1999) Space and attention in parietal cortex. Annu Rev Neurosci 22:319–349

Coull JT, Frith CD, Frackowiak RS, Grasby PM (1996) A fronto-parietal network for rapid visual information processing: a PET study of sustained attention and working memory. Neuropsychologia 34(11):1085–1095

de Groot M, Vernooij MW, Klein S, Ikram MA, Vos FM, Smith SM, Niessen WJ, Andersson JLR (2013) Improving alignment in Tract-based spatial statistics: evaluation and optimization of image registration. NeuroImage 76:400–411

Draganski B, Kherif F (2013) In vivo assessment of use-dependent brain plasticity-Beyond the "one trick pony" imaging strategy. NeuroImage 73:255–259

Draganski B, Gaser C, Busch V, Schuierer G, Bogdahn U, May A (2004) Neuroplasticity: changes in grey matter induced by training. Nature 427(6972):311–312

Eickhoff SB, Stephan KE, Mohlberg H, Grefkes C, Fink GR, Amunts K, Zilles K (2005) A new SPM toolbox for combining probabilistic cytoarchitectonic maps and functional imaging data. NeuroImage 25(4):1325–1335

Erickson KI (2013) Evidence for structural plasticity in humans: comment on Thomas and Baker (2012). NeuroImage 73:237–238

Evarts EV (1968) Relation of pyramidal tract activity to force exerted during voluntary movement. J Neurophysiol 31(1):14–27

Fields RD (2013) Changes in brain structure during learning: fact or artifact? Reply to Thomas and Baker. NeuroImage 73:260–264

Fieremans E, De Deene Y, Delputte S, Ozdemir MS, D'Asseler Y, Vlassenbroeck J, Deblaere K, Achten E, Lemahieu I (2008) Simulation and experimental verification of the diffusion in an anisotropic fiber phantom. J Magn Reson 190(2):189–199

Fieremans E, Deene YD, Baete S, Lemahieu I (2009) Design of anisotropic diffusion hardware fiber phantoms. Diffus Fundam 10:1–3

Gaser C, Schlaug G (2003) Brain structures differ between musicians and non-musicians. J Neurosci 23(27):9240–9245

Georgopoulos AP, Schwartz AB, Kettner RE (1986) Neuronal population coding of movement direction. Science 233(4771):1416–1419

Georgopoulos AP, Merchant H, Naselaris T, Amirikian B (2007) Mapping of the preferred direction in the motor cortex. Proc Natl Acad Sci USA 104(26):11068–11072

Goldberg G (1985) Supplementary motor area structure and function: review and hypotheses. Behav Brain Sci 8(04):567–588

Good CD, Johnsrude IS, Ashburner J, Henson RN, Friston KJ, Frackowiak RS (2001) A voxel-based morphometric study of ageing in 465 normal adult human brains. NeuroImage 14(1 Pt 1):21–36

Grabner RH, Ansari D, Koschutnig K, Reishofer G, Ebner F, Neuper C (2009) To retrieve or to calculate? Left angular gyrus mediates the retrieval of arithmetic facts during problem solving. Neuropsychologia 47(2):604–608

Grabner RH, Ansari D, Koschutnig K, Reishofer G, Ebner F (2013) The function of the left angular gyrus in mental arithmetic: evidence from the associative confusion effect. Hum Brain Mapp 34(5):1013–1024

Grill-Spector K, Kourtzi Z, Kanwisher N (2001) The lateral occipital complex and its role in object recognition. Vision Res 41(10–11):1409–1422

Griswold MA, Jakob PM, Heidemann RM, Nittka M, Jellus V, Wang J, Kiefer B, Haase A (2002) Generalized autocalibrating partially parallel acquisitions (GRAPPA). Magn Reson Med 47:1202–1210

Hahn B, Ross TJ, Stein EA (2006) Neuroanatomical dissociation between bottom–up and top–down processes of visuospatial selective attention. NeuroImage 32(2):842–853

Han Y, Yang H, Lv Y-T, Zhu C-Z, He Y, Tang H-H, Gong Q-Y, Luo Y-J, Zang Y-F, Dong Q (2009) Gray matter density and white matter integrity in pianists' brain: a combined structural and diffusion tensor MRI study. Neurosci Lett 459(1):3–6

Hänggi J, Koeneke S, Bezzola L, Jäncke L (2010) Structural neuroplasticity in the sensorimotor network of professional female ballet dancers. Hum Brain Mapp 31(8):1196–1206

Hasan MT, Hernández-González S, Dogbevia G, Treviño M, Bertocchi I, Gruart A, Delgado-García JM (2013) Role of motor cortex NMDA receptors in learning-dependent synaptic plasticity of behaving mice. Nat Commun 4. doi:10.1038/ncomms3258

Hayasaka S, Phan KL, Liberzon I, Worsley KJ, Nichols TE (2004) Nonstationary cluster-size inference with random field and permutation methods. NeuroImage 22(2):676–687

Hoeft F, Barnea-Goraly N, Haas BW, Golarai G, Ng D, Mills D, Korenberg J, Bellugi U, Galaburda A, Reiss AL (2007) More is not always better: increased fractional anisotropy of superior longitudinal fasciculus associated with poor visuospatial abilities in Williams Syndrome. J Neurosci 27(44):11960–11965

Iwamura Y, Tanaka M (1996) Representation of reaching and grasping in the monkey postcentral gyrus. Neurosci Lett 214(2–3):147–150

Jäncke L, Beeli G, Eulig C, Hanggi J (2009a) The neuroanatomy of grapheme-color synesthesia. Eur J Neurosci 29(6):1287–1293

Jäncke L, Koeneke S, Hoppe A, Rominger C, Hänggi J (2009b) The architecture of the Golfer's brain. PLoS One 4(3):e4785

Jones DK, Symms MR, Cercignani M, Howard RJ (2005) The effect of filter size on VBM analyses of DT-MRI data. NeuroImage 26(2):546–554

Jordan K, Wüstenberg T, Heinze H-J, Peters M, Jäncke L (2002) Women and men exhibit different cortical activation patterns during mental rotation tasks. Neuropsychologia 40(13):2397–2408

Keller TA, Just MA (2009) Altering cortical connectivity: remediation-induced changes in the white matter of poor readers. Neuron 64(5):624–631

Kennerley SW, Walton ME, Behrens TEJ, Buckley MJ, Rushworth MFS (2006) Optimal decision making and the anterior cingulate cortex. Nat Neurosci 9(7):940–947

Klein A, Andersson J, Ardekani BA, Ashburner J, Avants B, Chiang M-C, Christensen GE, Collins DL, Gee J, Hellier P, Song JH, Jenkinson M, Lepage C, Rueckert D, Thompson P, Vercauteren T, Woods RP, Mann JJ, Parsey RV (2009) Evaluation of 14 nonlinear deformation algorithms applied to human brain MRI registration. NeuroImage 46(3):786–802

Koechlin E, Ody C, Kouneiher F (2003) The architecture of cognitive control in the human prefrontal cortex. Science 302(5648):1181–1185

Kourtzi Z, Kanwisher N (2001) Representation of perceived object shape by the human lateral occipital complex. Science 293(5534):1506–1509

Kung C–C, Peissig JJ, Tarr MJ (2007) Is region-of-interest overlap comparison a reliable measure of category specificity? J Cogn Neurosci 19(12):2019–2034

Lee D, Quessy S (2003) Activity in the supplementary motor area related to learning and performance during a sequential visuo-motor task. J Neurophysiol 89(2):1039–1056

Leemans A, Jones DK (2009) The B1-matrix must be rotated when correcting for subject motion in DTI data. Magn Reson Med 61(6):1336–1349

Lloyd DM, Shore DI, Spence C, Calvert GA (2003) Multisensory representation of limb position in human premotor cortex. Nat Neurosci 6(1):17–18

MacEvoy SP (2013) "What?" and "where?" versus "what is where?": the impact of task on coding of object form and position in the lateral occipital complex. J Vis 13(8)

MacEvoy SP, Epstein RA (2011) Constructing scenes from objects in human occipitotemporal cortex. Nat Neurosci 14(10):1323–1329

Maguire EA, Gadian DG, Johnsrude IS, Good CD, Ashburner J, Frackowiak RSJ, Frith CD (2000) Navigation-related structural change in the hippocampi of taxi drivers. PNAS 97(8):4398–4403

Maitra R (2010) A re-defined and generalized percent-overlap-of-activation measure for studies of fMRI reproducibility and its use in identifying outlier activation maps. NeuroImage 50(1):124–135

May A, Gaser C (2012) Response to Thomas and Baker: the structural adaptation of the brain to training. Trends Cogn Sci 16(2):97–98

Mechelli A, Crinion JT, Noppeney U, O'Doherty J, Ashburner J, Frackowiak RS, Price CJ (2004) Neurolinguistics: structural plasticity in the bilingual brain. Nature 431(7010):757

Mechelli A, Price CJ, Friston KJ, Ashburner J (2005) Voxel-based morphometry of the human brain: methods and applications. Curr Med Imag Rev 1(2):105–113

Mori S, van Zijl PC (2002) Fiber tracking: principles and strategies-a technical review. NMR Biomed 15(7–8):468–480

Muellbacher W, Ziemann U, Wissel J, Dang N, Kofler M, Facchini S, Boroojerdi B, Poewe W, Hallett M (2002) Early consolidation in human primary motor cortex. Nature 415(6872):640–644

Nachev P, Kennard C, Husain M (2008) Functional role of the supplementary and pre-supplementary motor areas. Nat Rev Neurosci 9(11):856–869

Naito E, Ehrsson HH (2006) Somatic sensation of hand-object interactive movement is associated with activity in the left inferior parietal cortex. J Neurosci 26(14):3783–3790

Nichols TE, Holmes AP (2002) Nonparametric permutation tests for functional neuroimaging: a primer with examples. Hum Brain Mapp 15(1):1–25

Oechslin MS, Imfeld A, Loenneker T, Meyer M, Jäncke L (2009) The plasticity of the superior longitudinal fasciculus as a function of musical expertise: a diffusion tensor imaging study. Front Human Neurosci 3

Oh JS, Kubicki M, Rosenberger G, Bouix S, Levitt JJ, McCarley RW, Westin CF, Shenton ME (2009) Thalamo-frontal white matter alterations in chronic schizophrenia: a quantitative diffusion tractography study. Hum Brain Mapp 30(11):3812–3825

Oishi K, Zilles K, Amunts K, Faria A, Jiang H, Li X, Akhter K, Hua K, Woods R, Toga AW, Pike GB, Rosa-Neto P, Evans A, Zhang J, Huang H, Miller MI, van Zijl PCM, Mazziotta J, Mori S (2008) Human brain white matter atlas: identification and assignment of common anatomical structures in superficial white matter. NeuroImage 43(3):447–457

Pascual-Leone A, Amedi A, Fregni F, Merabet LB (2005) The plastic human brain cortex. Annu Rev Neurosci 28(1):377–401

Peelen MV, Kastner S (2011) Is that a bathtub in your kitchen? Nat Neurosci 14(10):1224–1226

Penfield W, Welch K (1951) The supplementary motor area of the cerebral cortex: a clinical and experimental study. AMA Arch Neurol Psychiatry 66(3):289–317

Pierpaoli C, Basser PJ (1996) Toward a quantitative assessment of diffusion anisotropy. Magn Reson Med 36(6):893–906

Radua J, Canales-Rodríguez EJ, Pomarol-Clotet E, Salvador R (2013) Validity of modulation and optimal settings for advanced voxel-based morphometry. NeuroImage (0). doi:10.1016/j.neuroimage.2013.07.084

Reese TG, Heid O, Weisskoff RM, Wedeen VJ (2003) Reduction of eddy-current-induced distortion in diffusion MRI using a twice-refocused spin echo. Magn Reson Med 49(1):177–182

Ridgway GR, Henley SM, Rohrer JD, Scahill RI, Warren JD, Fox NC (2008) Ten simple rules for reporting voxel-based morphometry studies. NeuroImage 40(4):1429–1435

Rivera SM, Reiss AL, Eckert MA, Menon V (2005) Developmental changes in mental arithmetic: evidence for increased functional specialization in the left inferior parietal cortex. Cereb Cortex 15(11):1779–1790

Rizzolatti G, Luppino G (2001) The cortical motor system. Neuron 31(6):889–901

Rizzolatti G, Matelli M, Pavesi G (1983) Deficits in attention and movement following the removal of postarcuate (area 6) and prearcuate (area 8) cortex in macaque monkeys. Brain 106(3):655–673

Rohde GK, Barnett AS, Basser PJ, Marenco S, Pierpaoli C (2004) Comprehensive approach for correction of motion and distortion in diffusion-weighted MRI. Magn Reson Med 51(1):103–114

Roland PE, Larsen B, Lassen NA, Skinhoj E (1980) Supplementary motor area and other cortical areas in organization of voluntary movements in man. J Neurophysiol 43(1):118–136

Scarpazza C, Sartori G, De Simone MS, Mechelli A (2013) When the single matters more than the group: very high false positive rates in single case voxel based morphometry. NeuroImage 70:175–188

Schlaug G, Forgeard M, Zhu L, Norton A, Winner E (2009) Training-induced neuroplasticity in young children. Ann N Y Acad Sci 1169:205–208

Schmahmann JD, Pandya DN, Wang R, Dai G, D'Arceuil HE, de Crespigny AJ, Wedeen VJ (2007) Association fibre pathways of the brain: parallel observations from diffusion spectrum imaging and autoradiography. Brain 130(Pt 3):630–653

Schmithorst VJ, Wilke M (2002) Differences in white matter architecture between musicians and non-musicians: a diffusion tensor imaging study. Neurosci Lett 321(1–2):57–60

Scholz J, Klein MC, Behrens TEJ, Johansen-Berg H (2009) Training induces changes in white-matter architecture. Nat Neurosci 12:1370–1371

Seghier ML, Fagan E, Price CJ (2010) Functional subdivisions in the left angular gyrus where the semantic system meets and diverges from the default network. J Neurosci 30(50):16809–16817

Shibasaki H, Sadato N, Lyshkow H, Yonekura Y, Honda M, Nagamine T, Suwazono S, Magata Y, Ikeda A, Miyazaki M, Fukuyama H, Asato R, Konishi J (1993) Both primary motor cortex and supplementary motor area play an important role in complex finger movement. Brain 116(6):1387–1398

Shima K, Tanji J (1998) Both supplementary and presupplementary motor areas are crucial for the temporal organization of multiple movements. J Neurophysiol 80(6):3247–3260

Silver M, Montana G, Nichols TE (2011) False positives in neuroimaging genetics using voxel-based morphometry data. NeuroImage 54(2):992–1000

Sluming V, Barrick T, Howard M, Cezayirli E, Mayes A, Roberts N (2002) Voxel-based morphometry reveals increased gray matter density in broca's area in male symphony orchestra musicians. NeuroImage 17(3):1613–1622

Smith SM, Nichols TE (2009) Threshold-free cluster enhancement: addressing problems of smoothing, threshold dependence and localisation in cluster inference. NeuroImage 44(1):83–98

Smith SM, Jenkinson M, Johansen-Berg H, Rueckert D, Nichols TE, Mackay CE, Watkins KE, Ciccarelli O, Cader MZ, Matthews PM, Behrens TEJ (2006) Tract-based spatial statistics: voxelwise analysis of multi-subject diffusion data. NeuroImage 31(4):1487–1505

Song W, Francis JT (2013) Tactile information processing in primate hand somatosensory cortex (S1) during passive arm movement. J Neurophysiol

Swick D, Ashley V, Turken AU (2008) Left inferior frontal gyrus is critical for response inhibition. BMC Neurosci 9:102

Takahashi M, Hackney DB, Zhang G, Wehrli SL, Wright AC, O'Brien WT, Uematsu H, Wehrli FW, Selzer ME (2002) Magnetic resonance microimaging of intraaxonal water diffusion in live excised lamprey spinal cord. Proc Natl Acad Sci USA 99(25):16192–16196

Tanaka S, Honda M, Sadato N (2005) Modality-specific cognitive function of medial and lateral human Brodmann area 6. J Neurosci 25(2):496–501

Tanji J (1994) The supplementary motor area in the cerebral cortex. Neurosci Res 19(3):251–268

Tanji J (1996) New concepts of the supplementary motor area. Curr Opin Neurobiol 6(6):782–787

Tanji J (2001) Sequential organization of multiple movements: involvement of cortical motor areas. Annu Rev Neurosci 24:631–651

Thomas C, Baker CI (2013a) On evidence, biases and confounding factors: response to commentaries. NeuroImage 73:265–267

Thomas C, Baker CI (2013b) Teaching an adult brain new tricks: a critical review of evidence for training-dependent structural plasticity in humans. NeuroImage 73:225–236

Thomas AG, Marrett S, Saad ZS, Ruff DA, Martin A, Bandettini PA (2009) Functional but not structural changes associated with learning: an exploration of longitudinal voxel-based morphometry (VBM). NeuroImage 48(1):117–125

Uddin LQ, Supekar K, Amin H, Rykhlevskaia E, Nguyen DA, Greicius MD, Menon V (2010) Dissociable connectivity within human angular gyrus and intraparietal sulcus: evidence from functional and structural connectivity. Cereb Cortex 20(11):2636–2646

Vaina LM, Solomon J, Chowdhury S, Sinha P, Belliveau JW (2001) Functional neuroanatomy of biological motion perception in humans. PNAS 98(20):11656–11661

van Veen V, Cohen JD, Botvinick MM, Stenger VA, Carter CS (2001) Anterior cingulate cortex, conflict monitoring, and levels of processing. NeuroImage 14(6):1302–1308

Vidoni ED, Acerra NE, Dao E, Meehan SK, Boyd LA (2010) Role of the primary somatosensory cortex in motor learning: an rTMS study. Neurobiol Learn Mem 93(4):532–539

Vinberg J, Grill-Spector K (2008) Representation of shapes, edges, and surfaces across multiple cues in the human visual cortex. J Neurophysiol 99(3):1380–1393

Wang B, Fan Y, Lu M, Li S, Song Z, Peng X, Zhang R, Lin Q, He Y, Wang J, Huang R (2013) Brain anatomical networks in world class gymnasts: a DTI tractography study. NeuroImage 65:476–487

Ward NS, Newton JM, Swayne OB, Lee L, Thompson AJ, Greenwood RJ, Rothwell JC, Frackowiak RS (2006) Motor system activation after subcortical stroke depends on cortico-spinal system integrity. Brain 129(Pt 3):809–819

Welberg L (2012) Visual system: How the brain distinguishes bugs from birds. Nat Rev Neurosci 11(1):223

Wenderoth N, Debaere F, Sunaert S, Hecke PV, Swinnen SP (2004) Parieto-premotor areas mediate directional interference during bimanual movements. Cereb Cortex 14(10):1153–1163

Yarrow K, Brown P, Krakauer JW (2009) Inside the brain of an elite athlete: the neural processes that support high achievement in sports. Nat Rev Neurosci 10(8):585–596

Zalc B, Douglas Fields R (2000) Do action potentials regulate myelination? Neuroscientist 6(1):5–13

Zalesky A (2011) Moderating registration misalignment in voxelwise comparisons of DTI data: a performance evaluation of skeleton projection. Magn Reson Imaging 29(1):111–125

Zatorre RJ, Fields RD, Johansen-Berg H (2012) Plasticity in gray and white: neuroimaging changes in brain structure during learning. Nat Neurosci 15(4):528–536

Zilles K, Amunts K (2010) Centenary of Brodmann's map—conception and fate. Nat Rev Neurosci 11(2):139–145